2018

Numerical Analysis of Fluid Flow and Heat Transfer in Wavy and Hybrid-Slit-Wavy (HSW) Fin-and-Tube Heat Exchangers

Lokanath Mohanta
UTC Climate Control and Security (Carrier Corp), United States of America, lokanath.mohanta@carrier.utc.com

Arindom Joardar
UTC Climate Control and Security (Carrier Corp), United States of America, Arindom.Joardar@carrier.utc.com

Jack Esformes
UTC Climate Control and Security (Carrier Corp), United States of America, Jack.Esformes@carrier.utc.com

Brian Videto
UTC Climate Control and Security (Carrier Corp), United States of America, Brian.Videto@carrier.utc.com

Tobias Sienel
UTC Climate Control and Security (Carrier Corp), United States of America, Tobias.H.Sienel@carrier.utc.com

Numerical Analysis of Fluid Flow and Heat Transfer in Wavy and Hybrid-Slit-Wavy (HSW) Fin-and-Tube Heat Exchangers

Lokanath Mohanta, A. Joardar, Jack L Esformes, Brian Videto and Tobias H. Sienel

UTC Climate, Control and Security (Carrier Corporation)
Heat Transfer Group, Technology & Components
6304 Thompson Road, Syracuse, NY.

ABSTRACT

This numerical study pertains to characterizing flow and heat transfer interactions for an interrupted fin design with wavy profile in compact tube-and-fin heat exchanger. Although designs with similar concept is prevalent in the HVAC&R industry not much literature exists on the subject combining wavy fins with periodic interruptions. Presently sinusoidal wavy fin is combined with slit fins to investigate thermal-hydraulic performance relative to an un-interrupted fin design. This fin is referred to as Hybrid Slit Wavy (HSW) fin in this work. Commercial Computational Fluid Dynamics (CFD) software is used for 3D numerical solution of the complete Navier–Stokes and energy equations in the heat exchanger to study flow physics and predict performance. The modeling approach is first validated with available test data from the literature on a wavy (Herringbone profile) fin heat exchanger. The predicted friction factor f was within 12% and the Colburn j-factor was within 7% of the reported test data over a Reynolds number range of 350-6500. In the case of the HSW fin it was found that the air-side heat transfer is enhanced by about 20-39% relative to the baseline un-interrupted fin with an associated pressure drop penalty of 20-38%. The area goodness factors of the HSW fins are up to 4 % higher compared to the wavy fins at various operating conditions indicative of favorable trade-off. It is further established that the local flow pattern including boundary layer modifications, wake structures and enhanced flow mixing correlates strongly with local Nusselt number distribution.

1. INTRODUCTION

Plate fin-and-tube heat exchangers find extensive use in wide variety of engineering applications including automotive, heating, ventilation and air-conditioning, refrigeration, aerospace, petrochemical, industrial processing, electronics, and food and beverage among others. In the case of air-to-liquid heat exchangers it is well known that the thermal performance is limited by the air-side thermal resistance which accounts for 65 to 85% of the overall resistance. As a result most performance improvement strategies reported in the literature are focused on developing enhanced fin surfaces to increase air-side heat transfer coefficient with minimal pressure drop penalty. In general there are two classes of enhancement techniques relative to a plain fin geometry: first is use of non-planar fins such as wavy, dimpled, and corrugated or herringbone type and the second class pertains to the interrupted fins such as louvered, offset-strip fin, lanced or slit and other novel concepts such as punched vortex generators. There is significant body of literature [1-2] that exists on each of these design concepts when applied individually.

There is a third category of enhanced fin surface geometries wherein the non-planar designs are combined with the fin interruptions. Although these hybrid designs are common in the industry [3] however not much open literature exists on the subject. The main objective of this numerical study is to evaluate the thermal-hydraulic performance of a sinusoidal wavy fin combined with slits and comparing to an un-interrupted Herringbone wavy (Corrugated) fin of similar dimension. This fin is referred to as Hybrid Slit Wavy (HSW) fin in this work. A brief overview of the relevant literature and outline of this work is detailed below.

The thermal-hydraulic performance of the wavy fin-and-tube heat exchangers has been studied both experimentally and, to lesser degree, numerically by several researchers. Kays and London [4] provided j

and *f* versus Re curves for two wavy fin geometries and compared their performance with an offset-strip fin. Wang et al. [5] tested 18 different wavy fin coils to study the influence of different geometrical parameters on performance. Jang and Chen [6] employed three-dimensional numerical simulations to investigate the heat transfer characteristics in multi-row wavy fin heat exchanger. Lately, Wang et al. [7, 8] provided the most updated thermal hydraulic correlations obtained by including all the previous data and new experimental results of wavy fin coils. Performance of slit type fin has also been presented by Wang et al. [9]. A comparison of plain, wavy and slit fin has been presented by Wen and Ho [10]. They found heat transfer performance is 3% higher for wavy fin and 13% higher for slit (compounded) fin in terms of Colburn *j*-factor with increase in *f*-factor by 27% and 70% for wavy and slit fins respectively.

The literature on the HSW type of fin geometries is quite limited. Yun et al. [11] performed wind-tunnel tests on six different HSW coils to characterize heat transfer and pressure drop performance. They reported higher heat transfer and pressure drop compared to smooth wavy fin geometry. To best knowledge the numerical modeling of the HSW fin geometries has not been reported. In this work three dimensional numerical model is developed to investigate the flow physics and performance characteristics of HSW fin heat exchanger relative to the wavy fin designs. First the modeling approach is validated on a wavy (Herringbone profile) fin geometry using experimental data from the literature [5]. The model is then used to predict the thermal-hydraulic performance of a state-of-the-art HSW fin design and a wavy fin configuration of similar pattern for comparative analysis. It may be noted that the wavy-fin geometry for validating the model is different from the one used for relative comparison with the HSW fin performance. In the latter case the wavy-fin had similar wave features and tube pattern as the HSW fin.

2. NUMERICAL METHOD

2.1 Geometry and Computational Domain

As mentioned above, the numerical model is validated with experimental data pertaining to the wavy fin-and-tube heat exchanger geometry as reported by Wang et al. [5]. Specifically the sample #6 is used and the dimensional details of the geometry are available in the reference and is not repeated here. Figure 1 presents the geometry of the HSW fin considered in this work. Also shown is the typical computational domain and the surface mesh. In this configuration there are three rows of tubes arranged in staggered arrangement. The collar diameter of the tube is (D_c) 7.46 mm, the transverse pitch (P_t) is 21.6 mm, longitudinal pitch (P_l) of 12.7 mm and there are 6 slits generating seven lances arranged in a wavy pattern. The slit-wavy pattern transitions to the circular collar in such a way that a flat region exists. This feature is also present in the wavy fin geometry. The middle slit has smallest transverse length and it increases for subsequent slits on either direction. The heat exchangers are usually fabricated by

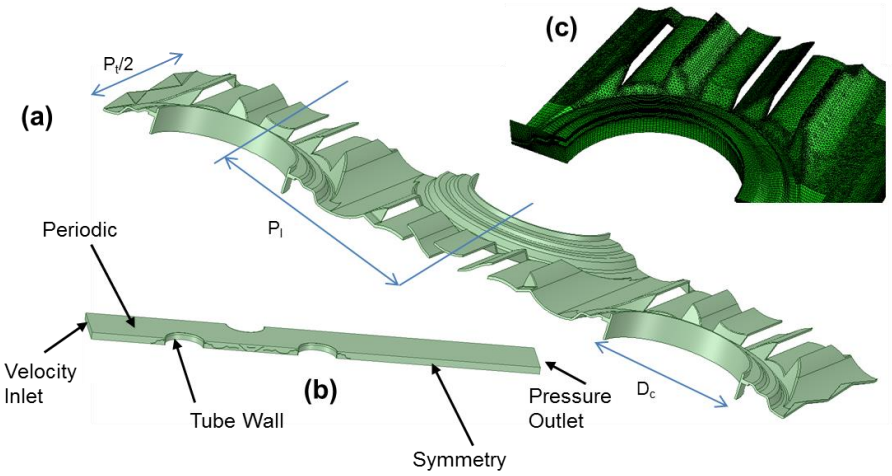

Figure 1. Geometry and computational domain (a) three row HSW fin geometry (b) computational domain with boundary conditions and (c) surface mesh.

mechanically expanding the tube in the fin-pack for ensuring a good contact between the tube and the collar. Therefore, thermal contact resistance between the tube and the collar is neglected in the current analysis. The computational domain models a set of three tubes as shown in Fig. 1(b), spanning from the inlet to the exit face of the heat exchanger. A back environment region is also added since the flow is recovering in the exit region. An inlet plenum is added to allow for flow to develop before entering the fins. The computational mesh is generated using ICEM CFD software and a combination of hexahedral and tetrahedral elements is used as shown in the Fig. 1(c).

2.2 Solver and Boundary Conditions

The three-dimensional Reynolds Averaged Navier–Stokes (RANS) and energy equation along with the relevant boundary conditions are solved as conjugate formulation using the commercial finite-volume based solver—Fluent 18.1. The governing equations in conservative form are discretized with finite-volume formulation using a fully implicit second-order upwind differencing scheme. The shear-stress transport (SST) κ-ω model is used to model the Reynolds stress terms and achieve closure of RANS equations. In the literature, researchers [12-14] have used different turbulence models as well as laminar flow assumption to model interrupted fin geometries and there is no clear evidence of one particular model being superior to others. In this study the κ-ω (SST) model provided best accuracy for the model validation runs with wavy fin and was retained for HSW fin modeling as well. The summary of major model assumptions are listed below:

- Steady-state incompressible flow
- Density of air is function of temperature only and no dependence on pressure
- Symmetry boundary condition through the plane intersecting tube-center axially
- The tube wall is assumed to be at constant temperature
- Negligible thermal contact resistance between tube and collar

An overview of the boundary conditions used in various zones of the CFD model is shown in Fig. 1(b) above. A uniform velocity and constant temperature boundary condition is used at the inlet of the computational domain. The air inlet temperature and tube wall temperatures come from the experimental data [5]. A zero gauge pressure boundary condition is set at the outlet. The top and bottom face of the computational domain are set as periodic. The side faces are set as symmetric planes

2.3 Data Reduction

The CFD model predicts the overall heat transfer rate and pressure drop performance of the heat exchanger configuration. The well-known *ε—NTU* method is used to reduce the data to obtain the non-dimensional Colburn *j*-factor and the friction *f*-factor as detailed below. This method closely follows the procedure used by Wang et al. [5] to reduce their experimental data. It may be noted that in the CFD model the tube wall temperature is constant for which $C_{min}/C_{max} = 0$. Hence for this condition the effectiveness (ε) is related to *NTU* in the following manner.

$$\varepsilon = 1 - e^{-NTU} = \frac{T_{out} - T_{in}}{T_{wall} - T_{in}} \tag{1}$$

Where, T_{in} and T_{out} are air inlet and exit temperatures and T_{wall} is the tube-side temperature. The overall thermal resistance based on total external surface area (A_o) for the fin-tube configuration can be defined as,

$$\frac{1}{U_O A_O} = \frac{\delta_w}{k_w A_w} + \frac{1}{\eta_O h_O A_O} \tag{2}$$

where η_O is the overall surface efficiency, U_o is overall heat transfer coefficient, k_w is thermal conductivity of tube, δ_w is tube wall thickness and A_w is tube internal surface area. The fin efficiency is calculated using the Schimdt [15] approximation. The Nusselt Number (*Nu*) and Reynolds number (Re_{Dc}) is calculated based on the fin collar diameter. The air-side heat transfer characteristic expressed as the Colburn *j*-factor is given by,

$$j = \frac{Nu}{Re_{D_c} Pr^{1/3}} \tag{3}$$

where, *Pr* is Prandtl number. The core friction factor is calculated following the method proposed by Kays and London [4], which accounts for the entrance and exit losses present in the CFD model.

$$f = \frac{A_c}{A_0}\frac{\rho_m}{\rho_1}\left[\frac{2\rho_1 \Delta P}{G_c^2} - (K_c + 1 - \sigma^2) - 2\left(\frac{\rho_1}{\rho_2} - 1\right) + (1 - \sigma^2 - K_c^2)\frac{\rho_1}{\rho_2}\right] \quad (4)$$

where ρ_1, ρ_2 and ρ_m are air inlet, outlet and mean density respectively, K_c is loss coefficient, A_c is cross-sectional area, ΔP is pressure drop, G_c is mass-flux and σ is the ratio of free flow area to frontal area. The entrance and exit loss factors are estimated using Fig. 5.2 of the reference ibid.

2.4 Model Validation

The issues of numerical accuracy and resolution are important for any computational model for complex flows. The three-dimensional HSW fin geometry has the potential for generating highly complex velocity and thermal fields. Hence the veracity of the overall modeling approach and adequacy of the grid resolution need to be ascertained in order to quantify the predictive capabilities. The grid independency aspects are covered in the next section. In this section the predicted overall heat transfer performance and pressure drop is compared to the experimental results from the literature for $350<Re_{Dc}<6000$. This corresponds to $90<Re_h<2000$ where Re_h is Reynolds number based on hydraulic diameter. For this purpose the work reported by Wang et al. [5] is used and in particular the measured performance of sample #6 is chosen for comparison with the numerical model. This wavy fin-and-tube heat exchanger is two row configuration with 10.3 mm outer tube diameter, fin pitch of 2.34 mm, transverse and longitudinal pitches of 25.4 mm and 19.05 mm respectively. The Colburn *j* factor and friction factor predictions are compared to the measured results in Fig. 2. The deviation of predicted *j* factor from the test data is 2% at Re_{Dc}=750 and around 7% at Re_{Dc}= 6400. Similarly the friction factor discrepancy is 12 % at low Re and about 4% at Re_{Dc}=6400. The agreement between the predicted and measured thermal-hydraulic performances is considered very good for the given range of operating conditions and is indicative of the predictive capability of the overall modeling approach. In addition to the experimental results, a correlation for wavy fin geometries developed by Wang et al. [7] is also compared against the test data in Fig. 2. The correlation for Colburn factor predicts the test data with good accuracy (within 13%). However, the accuracy of the friction factor is very poor with errors larger than 50%. This could be due the erroneous formula (Eq. (1) of [7] vs. [4] above) used by the authors to reduce the friction factor data and possibly due to the neglect of the entry and exit losses as well. The Eq. (1) of Wang et al.[7], the ratio of $\frac{\rho_m}{\rho_1}$ is inverted and ρ_1 is divided in the first term instead of multiplication.

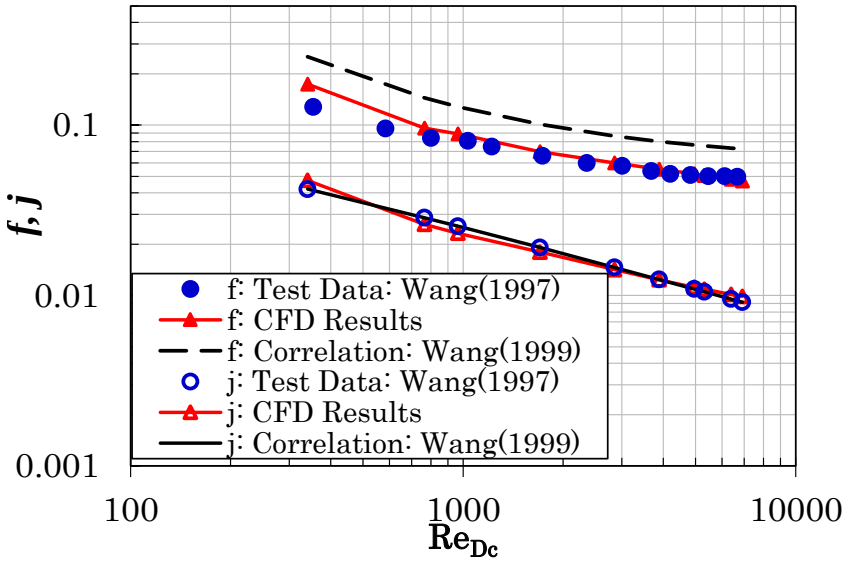

Figure 2. Computed and experimental (from Ref. [5]) comparison in terms of Colburn j-factor and friction factor.

2.5 Grid Independency

Non-uniform mesh with hexahedral and tetrahedral cells is used to discretize the computational domain. For the wavy fin geometry four different mesh sizes were evaluated to verify that numerical solution obtained is grid independent. In all the meshes the y^+ is maintained below 2. Grid resolutions with cell count from 4.2×10^5 to 1.4×10^6 are used for the simulation of wavy-fin validation model. The impact of mesh count on the overall performance is summarized in Fig. 3 below. It can be seen that the simulation results are fairly insensitive for cell counts larger than about 6×10^5. So the final cell count of about 6×10^5 is used for modeling the two wavy-fin geometries that appear in this work. In the case of the HSW fin geometry only two different grid resolutions (3×10^6 and 4×10^6) are simulated due to paucity of computational resources and results are found to be insensitive between the two cell counts.

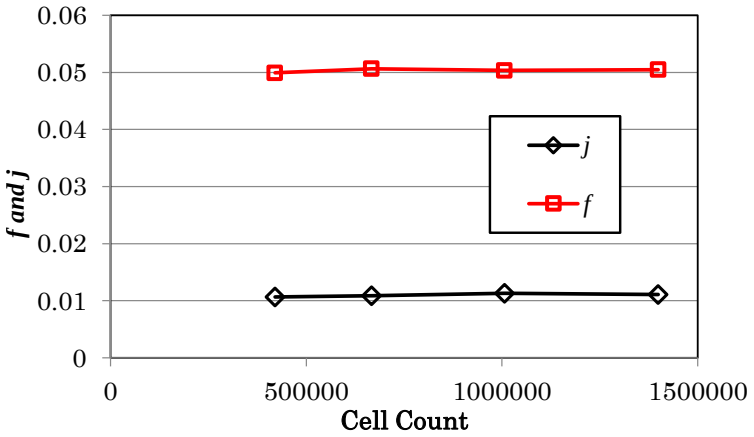

Figure 3. CFD results as function of grid size for the baseline wavy fin geometry

3. RESULTS AND DISCUSSION

In this section the flow and heat transfer behavior of the wavy fin and HSW fin-and-tube heat exchanger configurations are presented for Re_{Dc}=2200 which is equivalent to R_h=520. As alluded before, in order to compare the performance of the two geometries on equal footing the wavy fin used for model validation was scaled to match the HSW design in terms of the collar diameter, row count, wave height, fin pitch, transverse tube pitch and the longitudinal row pitch. Prior to examining the thermal-hydraulic performance of the two configurations, it is useful to analyze the dominant flow structures relevant to pressure drop and heat transfer in these heat exchangers. Details of the local flow patterns and local heat transfer characteristics are discussed in the following subsections. Finally, overall heat transfer and pressure drop results are presented for $350<Re_{Dc}<6000$ which corresponds to $90<Re_h<2000$.

3.1 Fluid Flow Behavior

Typical flow pattern in wavy fin-and-tube geometry is depicted in Figs. 4(a) and (b) in terms of pathlines and mid-plane streamline profiles respectively colored by the velocity magnitude. An effective way to visualize the flow is to consider the numerically generated pathlines, as shown in Fig. 4(a), capturing the wavy motion associated with the fin geometry and modified by the presence of the staggered tube pattern. As the oncoming flow enters the fin-pack the fluid periodically accelerates due to the confinement effects of the tube and decelerates while transitioning from one row to the next. As expected it can be clearly seen that the maximum local velocity at the convex tube wall occurs at minimum flow cross-sectional area of the first tube row. As the flow leaves the first row it tends to recover in the downstream region but encounters stagnant flow zones at trailing end of first tube and leading edge of the second row tube as shown in Fig. 4(b). As a result the effective cross-sectional area available is diminished depending on the size of the recirculation zones leading to relatively high local velocities in the transition zone. The structure and circulation strength of the stagnant zones are strongly dependent on the operating Reynolds number and the tube spacing's in either directions. Also the spatial

extent of the recirculation zone varies from the entrance row to the exit row. The tubes with no immediate downstream neighbor have larger recirculation zones compared to the ones in the interior with downstream neighbor. The stagnant flow regions in the tube wake, formed due to flow separation effects, has profound influence on the local convective heat transfer as discussed quantitatively in later section.

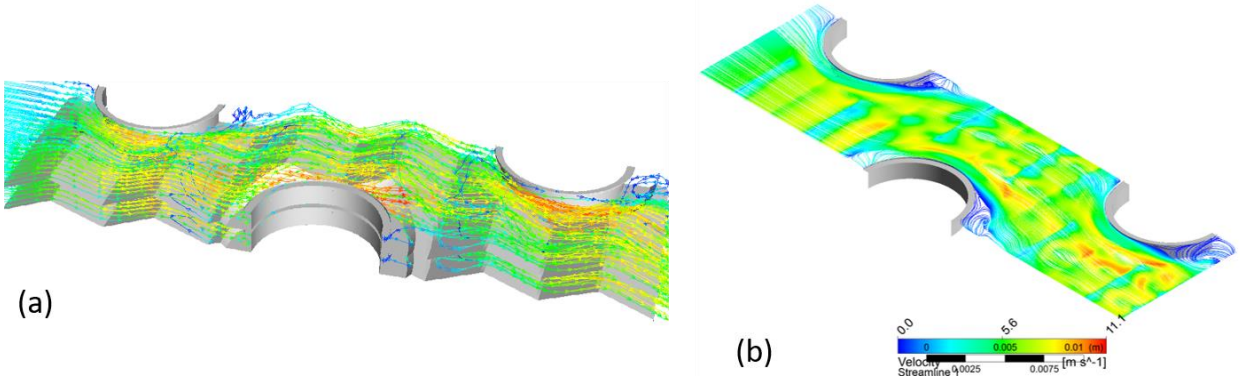

Figure 4. Flow pattern for the scaled wavy-fin geometry as shown by the (a) pathlines and (b) streamlines plots in mid-plane colored by velocity magnitude. The air flow direction is from left to right.

The cross-sectional streamline plot in Fig. 5 further illustrates the flow physics of the herringbone wavy fin-and-tube heat exchanger. It is known [17] that for pure wavy channel flows at low Re number the viscous forces dominate and a streamline, fully developed duct flow type behavior prevails. This effect diminishes at higher Re numbers and boundary-layer separation downstream of corrugation peaks gives rise to a vortex flow structure in the valley region. It appears that the general flow behavior in the wavy fin-and-tube heat exchangers is somewhat analogous to the pure wavy duct flow. As seen in Fig. 5, the boundary-layer separation and recirculation zones are prominent locally in transition regions between two tubes where the flow is not influenced by the presence of the tubes. These effects are significantly suppressed in fin areas where tube is present. However the effects of upstream flow separation are expected to influence the downstream flow structure despite suppression by the tubes. The recirculation at peak and valley is enveloped in the near-wall flow separation bubble which act to accelerate core flow locally. The boundary-layer modifications, local fluid mixing and core flow acceleration all act to enhance convective heat transfer, although the associated flow friction also increases which manifest as pressure drop penalty.

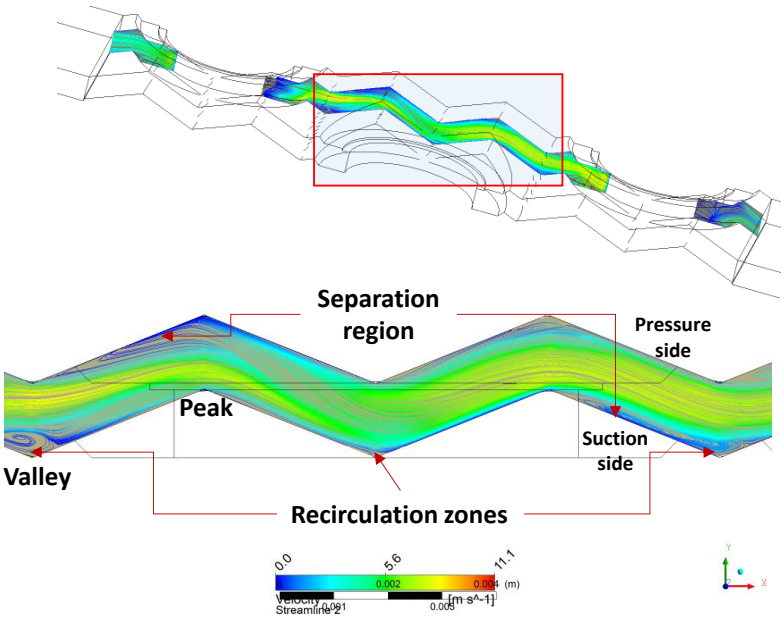

Figure 5. Cross sectional streamline plot showing flow pattern for the scaled wavy-fin geometry.

The fluid flow characteristics for the HSW fin-and-tube heat exchanger is shown in Figs. 6(a) and (b) in terms of pathlines and mid-plane velocity contour plot. As discussed before the fin cross sectional profile is sinusoidal which is the usual practice in this class of heat exchanger designs primarily in the HVAC applications. The fin interruptions fashioned by the multiple slits along the flow direction act to restart the boundary-layer periodically and enhance the convective heat transfer performance. The individual slits are of varying lengths—the shortest ones are diametrically opposite to the tube and the longest ones are in the vicinity of the leading or trailing end of the tubes. There is a relatively flat transition zone around the tube circumference, similar to the wavy fin, between the continuous fin-collar and the wavy-slits. The overall fluid flow behavior is impacted by the relative proportion of this flat transition area. Higher proportion of air mass flow is expected for larger transition areas due to relatively lower resistance compared to the wavy-slit areas. This can be discerned in Fig. 6 where high local velocities is clearly seen in the flat transition zone around the tubes. In general the local flow behavior around the tube-collar is similar to the well-known flow around finned cylinder. Presence of recirculation in the tube wake areas is also expectedly observed. As alluded before these stagnant zones lead to poor local convective heat transfer performance.

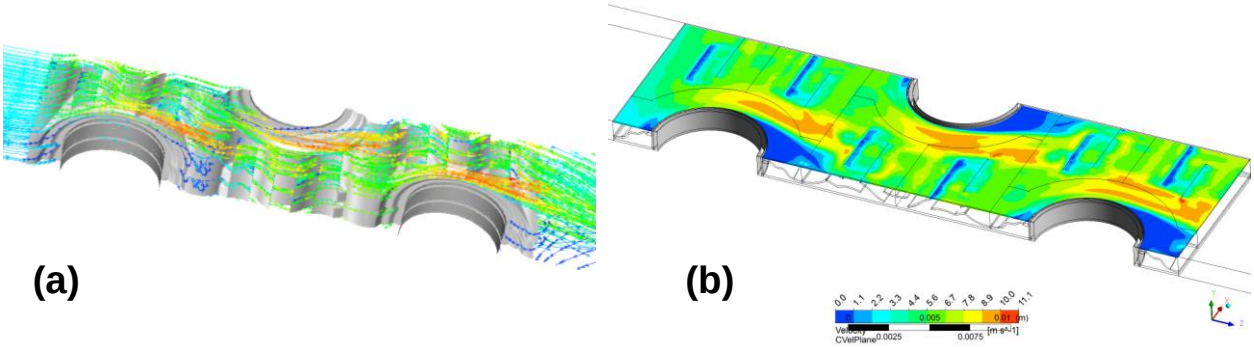

Figure 6. Flow pattern for the HSW fin geometry as shown by the (a) pathlines and (b) velocity contour plot in mid-plane section. The air flow direction is from left to right.

The local flow in the wavy channel modified by the slit interruptions is fairly complex in a staggered tube heat exchanger configuration. A comprehensive discussion is not attempted here and the intent is to highlight some basic features which have a bearing on the heat transfer performance. The cross-sectional streamline plot in Fig. 7 is instructive to study the local flow field. Because the slits are formed from the sinusoidal wavy channel they have an inherent curvature and the flow around the slit-elements formed at the peak and valley regions behave analogous to an airfoil. Recirculation zones on the

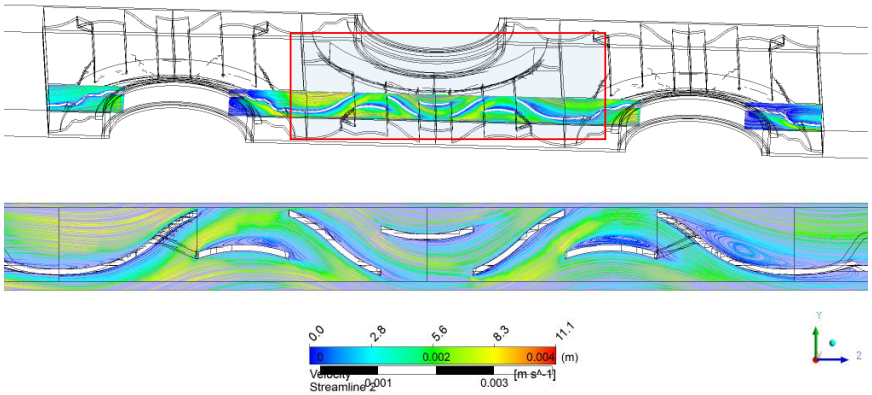

Figure 7. Cross sectional streamline plot showing flow pattern for the HSW fin geometry

convex side is clearly visible. Interestingly, in some other areas of the fin the recirculation zones appear on the concave side. This difference is primarily related to the incidence angle of the oncoming flow and the slit orientation. Furthermore it is important to note that the slits split the flow and the downstream slits are unlikely to be influenced by the thermal wake of the upstream slits. This is the major advantage of the HSW fins compared to the plain interrupted fins.

3.2 Local Nusselt Number Distribution

The comparative analysis of the local heat transfer behavior between the wavy and HSW fin is facilitated with reference to the local normalized Nusselt number distribution presented in Fig. 8(a) and (b). The normalized Nusselt number is the ratio of local Nusselt number to the air-side area weighted average Nusselt number ($\overline{Nu} = Nu_l/Nu_{avg}$). The local Nusselt number is calculated using the local wall heat flux, local wall temperature and inlet air temperature as the reference temperature ($Nu_l = \frac{hD_c}{k}$, $h = q_w^{"}/(T_w - T_{in})$ and $Nu_{avg} = \int Nu_l dA/\int dA$). The results presented in Fig. 8 are at a Reynolds number of approximately 520 based on the hydraulic diameter for both fins. As expected the normalized Nusselt number is highest at the leading edges of the fin where the boundary-layer is thin and high heat transfer driving potential. Zones of relatively high local Nusselt number are also visible the near the upstream-side periphery of the tubes. The normalized Nusselt number is close to zero at the downstream side of the tube due to the stagnant recirculation wakes mentioned before. As seen in Fig. 8(a), for wavy fins there is a pattern of alternating bands of high and low heat transfer corresponding to the uphill and downhill faces. As mentioned before this is related to the near-wall flow separation on downhill (suction) faces, shown in Fig. 5, which results in poor convective heat transfer. The high convective heat transfer on the pressure faces is primarily due to boundary layer thinning and accelerated core flow as discussed before. In case of HSW fins, the normalized Nusselt number is very high at the leading edges of each slit due to boundary-layer restart effects as shown in Fig. 8(b). The slits also promote mixing and act to destabilize the flow [16] which result in enhanced convective thermal performance.

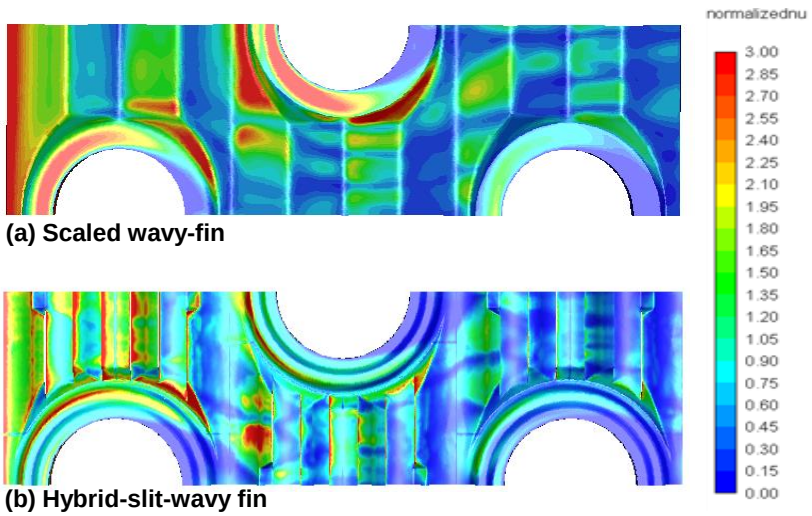

Figure 8: Normalized Nusselt Number comparisons at a Re_{Dc}=2200.

3.3 Overall Thermal-hydraulic Performance: Wavy vs. HSW Fin

The thermal hydraulic performances of the wavy and HSW fin configurations are compared in terms of friction *f*-factor and Colburn *j*-factor as shown in Fig. 9. On average, the Colburn *j*-factor for HSW fin is 22 to 40 % higher compared to the equivalent herringbone wavy fin over the range of Reynolds number 80-1400 based on the hydraulic diameter. The convective thermal performance of the HSW fin is expectedly superior to the wavy fin and is attributed to the flow modifications by the fin

interruptions superimposed on the wavy profile as discussed previously The enhanced thermal performance of HSW fins is associated with 20 to 40% increase in the friction factor as well which manifest as pumping power penalty. In low-Re flow operating conditions in compact heat exchangers usually the heat transfer augmentation has greater impact on system performance than the pressure drop penalty. Because of such enhancements a heat exchanger with HSW fin can be smaller in size for the same heat duty. The available size reduction could be redeemed by reducing the flow length (and hence reducing the pressure penalty) and can reduce cost and allow more compactness. One of the popular performance-evaluation-criterion in the literature to compare different heat exchanger performances is the area goodness factor or the *j/f* ratio. The area goodness factor for the HSW fin is up to 4 % higher than the equivalent herringbone wavy fin.

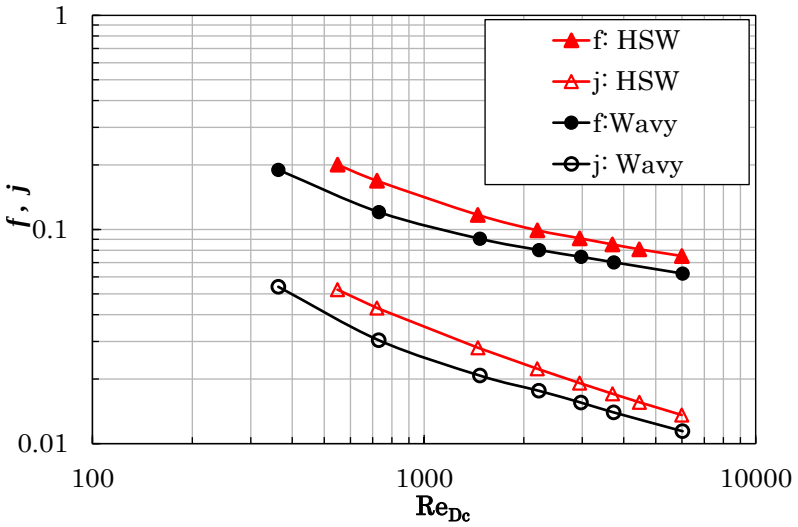

Figure 9. Thermal-hydraulic performance of the scaled wavy and HSW fin-and-tube heat exchangers

4. CONCLUSIONS

In this work three dimensional CFD based modeling procedure was used to investigate flow and heat transfer interactions in wavy and Hybrid Slit Wavy (HSW) fin-and-tube heat exchanger configurations. The modeling approach is first validated with available test data from the literature on a wavy (Herringbone profile) fin heat exchanger. The predicted friction factor *f* was within 12% and the Colburn *j*-factor was within 7% of the reported test data over a Reynolds number (based on collar diameter) range of 350-6500. The modeling approach was then deployed to study flow physics and predict performance of the HSW fin geometry. Stagnant flow exists in tube wake regions with negligible convective heat transfer. Recirculation zones were also found at the peak and valley regions of the wavy fins which act to accelerate core flow locally. In the HSW fin flow, the slits interrupted the flow periodically and local recirculation zones were found on one side or the other of the slits depending on their orientation relative to the flow incidence angle. The dominant enhancement mechanism for HSW fins are related to the periodic boundary-layer restart, local fluid mixing and core flow acceleration. The convective heat transfer enhancement is accompanied with increased flow friction which manifest as pressure drop penalty. In the case of the HSW fin it was found that the air-side heat transfer is enhanced by about 20-39% relative to the baseline un-interrupted fin with an associated pressure drop penalty of 20-38%. The area goodness factors of the HSW fins are up to 4 % higher compared to the wavy fins at various operating conditions indicative of favorable trade-off. It is envisaged that high fidelity numerical modeling approach as presented in this work could be a powerful tool for heat exchanger design and optimization efforts. Further research efforts are needed over wider range of operating conditions and to understand the impact of different design parameters on the thermal-hydraulic performance of HSW fins.

5. REFERENCES

1. Bhuiyan, A.A., Sadrul Islam, A.K.M., (2016) "Thermal and hydraulic performance of finned-tube heat exchangers under different flow ranges: A review on modeling and experiment." *International Journal of Heat and Mass Transfer* 101: 38–59
2. Wang C.C., (2000) "Recent progress on the air-side performance of fin-and-tube heat exchangers." *International Journal of Heat Exchangers*, 1(1):49–76
3. Sacks, P.S., "Lanced sine wave heat exchanger." United States patent US 4860822 Aug 29, 1989
4. Kays, W.M., London, A.L., (1984) Compact Heat Exchangers, McGraw-Hill, New York.
5. Wang, C.C., Fu, W.L., Chang, C.T., (1997) "Heat transfer and friction characteristics of typical wavy-fin and-tube heat exchangers." *Experimental Thermal Fluid Science* 14(2):174–86.
6. Jang J.Y., Chen, L.K., (1997) "Numerical analysis of heat transfer and fluid flow in a three dimensional wavy-fin and tube heat exchanger" *International Journal of Heat and Mass Transfer* 40(16): 3981–90.
7. Wang, C.C., Jang, J.Y., and Chiou, N.F., (1999) "Technical Note A heat transfer and friction correlation for wavy fin-and-tube heat exchangers." *International journal of heat and mass transfer* 42(10): 1919-1924
8. Wang, C.C, Hwang, Y.M, Lin, Y.T., (2002) "Empirical correlations for heat transfer and flow friction characteristics of herringbone wavy fin-and-tube heat exchangers" *International Journal of Refrigeration*, 25(5):673–80.
9. Wang, C.C., Tao, W.H., Chang, C.J. (1999) "An investigation of the airside performance of the slit fin-and-tube heat exchangers." *International Journal of Refrigeration* 22(8): 595-603.
10. Wen, M.Y., Ho, C.Y., (2009) "Heat-transfer enhancement in fin-and-tube heat exchanger with improved fin design." *Applied Thermal Engineering* 29(5-6): 1050-1057.
11. Yun, J.H., Peck, J.H., Kim, N.H, Kim, J.S., Lee, S.G., Nam, S.B., Kwon, H.J., (1997) "Heat transfer and friction characteristics of the fin-and-tube heat exchangers with slit-wavy fin" *International Journal of Air Conditioning & Refrigeration* 5: 162–170.
12. Lu, C.W., Huang, J.M., Nien, W.C., Wang, C.C., (2011) "A numerical investigation of the geometric effects on the performance of plate finned-tube heat exchanger." *Energy Conversion and Management* 52(3): 1638-1643.
13. Kumar, A., Joshi, J.B., Nayak, A.K., (2017) "A comparison of thermal-hydraulic performance of various fin patterns using 3D CFD simulations." *International Journal of Heat and Mass Transfer* 109: 336-356.
14. Ricardo, R.M., Sen, M., Yang, K.T., and McClain, R., (2000) "Effect of fin spacing on convection in a plate fin and tube heat exchanger." *International Journal of Heat and Mass Transfer* 43 (1): 39-51.
15. Schmidt, Th E., (1949) "Heat transfer calculations for extended surfaces." *Refrigeration Engineering* 57(4): 351-357.
16. Wu, H.L., Gong, Y., Zhu, X., (2007) "Air flow and heat transfer in louver-fin round-tube heat exchangers" *ASME Journal of Heat Transfer* 129 (2): 200-210
17. Zhang, J., Kundu, J., Manglik., R.M., (2004) "Effect of fin waviness and spacing on the lateral vortex structure and laminar heat transfer in wavy-plate-fin cores." *International Journal of Heat and Mass Transfer* 47: 1719–1730.